PHOTOSYNTHETICA
International Journal for Photosynthesis Research

DOI 10.32615/ps.2025.029 PHOTOSYNTHETICA 63 (4): 309-321, 2025

Spectral light quality differentially modulates PSII energy partitioning among soybean genotypes

M. MARTÍNEZ-MORÉ[*,**], S. SIMONDI[***], M.M. SAINZ[#], V. BONNECARRÈRE[##], S. FERNÁNDEZ[###], and G. QUERO[*,+]

Photobiology Laboratory, Department of Plant Biology, Faculty of Agronomy, Universidad de la República, Garzón 809, Montevideo, Uruguay[*]
Department of Crop Sciences, University of Illinois, Urbana, Illinois, USA[**]
Mathematics Area, Faculty of Exact and Natural Sciences, Universidad Nacional de Cuyo (FCEN-UNCuyo), Padre Contreras 1300, Mendoza, Argentina[***]
Biochemistry Laboratory, Department of Plant Biology, Faculty of Agronomy, Universidad de la República, Garzón 809, Montevideo, Uruguay[#]
Instituto Nacional de Investigación Agropecuaria (INIA), Plant Genetic Improvement and Biotechnology Area, Wilson Ferreira Aldunate Experimental Station, Ruta 48, Km 10, Rincón del Colorado, 90200, Canelones, Uruguay[##]
Faculty of Engineering, Institute of Electrical Engineering, Universidad de la República, Julio Herrera y Reissig 565, Montevideo, Uruguay[###]

Abstract

Cultivated soybean is a globally important crop; understanding its responses to different light spectra within the canopy is essential, especially considering the limited agricultural area. Energy flux and spectral quality are key components of the light environment that determine photosynthesis and, consequently, plant growth. These factors influence the composition and structure of photosystem II, thereby affecting energy partitioning between photochemical and nonphotochemical processes. This study evaluated the photosynthetic performance of two soybean genotypes under four light environments with distinct spectral compositions but equal energy flux. Results showed that PSII efficiency improved by the wavelengths outside the PAR range, irrespective of genotype. However, quantum yield parameters revealed genotype-specific responses under blue and red light. Plants exposed exclusively to red light exhibited reduced photosynthetic efficiency and increased photodamage after prolonged exposure, consistent with red light syndrome.

Keywords: *Glycine max*; photosystem II; quantum yields; quenching analysis; red light syndrome; relaxation analysis.

Highlights

- Wavelengths outside the PAR range improve the operating efficiency of PSII
- The red light syndrome induced reduction in the maximum quantum efficiency of PSII
- In soybean, there is a genotype-specific sensitivity to blue light and red light

Received 17 July 2025
Accepted 23 September 2025
Published online 20 October 2025

[+]Corresponding author
e-mail: gastonquero@fagro.edu.uy

Abbreviations: BL – LED-blue light; DSAL – defined spectrum actinic light; E_e – energy flux; F – fluorescence induction; F_0 – minimum fluorescence in the initial phase; F_0' – minimum fluorescence in the quenching analysis phase; F_0'' – minimum fluorescence in the relaxation analysis phase; F_m – maximum fluorescence in dark conditions; F_m' – maximum fluorescence in light conditions; F_m'' – maximum fluorescence in dark conditions during recovery; FR – far-red light pulse; F_t – fluorescence for light-adapted states in the time t; G – genotype; LED – light-emitting diode; LT – light treatment; MH – metal halide lamps; $P_{e\lambda}$ – spectral power; Q_A – plastoquinone A; q_P – fraction of open PSII centers at the time t; RC – reaction center; RH – relative humidity; RL – LED-red light; RWL – LED-red light-enriched white light; SP – saturating pulses; SSI – spectral susceptibility index; VPD – vapor pressure deficit; WL – MH-white light; Φ_{NO} – quantum yield of constitutive or basal nonphotochemical quenching; Φ_{NOa} – basal quantum yield of thermal dynamic dissipation within PSII when the pool of Q_As is partially oxidized or partially reduced; Φ_{NOb} – basal quantum yield of thermal dissipation within PSII in dark-adapted conditions when Q_A is fully oxidized; Φ_{NPQ} – quantum yield of regulatory light-induced nonphotochemical quenching; Φ_{NPQf} – quantum yield of the nonphotochemical quenching of rapid relaxation; Φ_{NPQs} – quantum yield of the nonphotochemical quenching of slow relaxation; Φ_{PSII} – quantum yield of the PSII; $\Phi_{PSIIpot}$ – maximal quantum yield of PSII photochemistry for the light-adapted state.

Acknowledgements: This research was funded by Comisión Sectorial de Investigación Científica (CSIC) Project named "Research Equipment Enhancement Program UDELAR-CSIC-2021-026".

Conflict of interest: The authors declare that they have no conflict of interest.

Introduction

Cultivated soybean is one of the most important crops worldwide. Currently, it is the primary source of protein and oil for human and animal feed and is becoming one of the most economically important biodiesel crops (Hartman *et al*. 2011, Zhang *et al*. 2022). With limited agricultural land and an increasing human population, it is necessary to improve soybean yields by generating new genetic material and optimizing agricultural practices, such as planting density (Stirbet *et al*. 2020). To enhance plant density in a crop, it is crucial to understand how genotypes respond to different wavelength ranges as the spectral composition of light changes within the canopy (Skálová *et al*. 1999, Courbier and Pierik 2019).

The light environment for plant development is defined by several factors, including the quantity (*i.e*., intensity and photoperiod) and quality (*i.e*., spectral composition) of light (Devlin *et al*. 2007, Zheng and Van Labeke 2017, Quero *et al*. 2021). This environment defines photosynthesis in plant cells by affecting leaf anatomy, the composition and structure of the light-harvesting complexes (the antenna), and the photosystem as a whole (Hogewoning *et al*. 2010a, Lazar *et al*. 2022, Didaran *et al*. 2024). These conditions must be taken into account when photosynthesis studies are carried out using artificial growth conditions.

Various lighting systems, such as metal halide, high-pressure sodium, incandescent, and white fluorescent lamps, are commonly used in these studies (Kochetova *et al*. 2022). In recent years, light-emitting diode (LED) lighting systems have emerged as a very advantageous technology for studying photosynthesis in plants, because they emit a narrow-band light (10–30 nanometers), which is suitable to ensure plant development (Yudina *et al*. 2022, Sena *et al*. 2024). The utilization of narrow-band LED light, which deviates significantly from natural light spectra, has been observed to induce alterations in the photosystems of plants, and consequently in the photosynthetic efficiency (Kochetova *et al*. 2022).

Photosynthetic efficiency refers to the conversion of light into chemical energy in plants. At the PSII level, it is commonly assessed through quantum yield parameters, which vary with light quality and intensity and indicate whether absorbed energy is used in photochemistry or dissipated as heat (Hogewoning *et al*. 2010b, Hamdani *et al*. 2019, Fang *et al.* 2021).

The effect of light quality on plant development has been largely studied using a growing light environment made up of different combinations of blue and red or white light (Yorio *et al.* 2001, Matsuda *et al.* 2004, Ohashi-Kaneko *et al.* 2006, Yudina *et al*. 2022).

The effect of blue and red light has been widely studied since the absorption spectra of photosynthetic pigments are mainly in the 400–450 nm and 600–700 nm wavelength intervals (Wang *et al.* 2016, Trivellini *et al.* 2023). Blue light optimizes photosynthesis by improving light capture efficiency (Takemiya *et al.* 2005, Zheng and Van Labeke 2017) and increasing the proportion of open reaction centers (RC) (Yang *et al.* 2017, Zheng and Van Labeke 2018, Fang *et al.* 2021). However, it was reported that blue light also causes PSII photodamage because it affects the Mn-cluster of the oxygen-evolving complex (Zavafer *et al.* 2015a, Zavafer 2021). Conversely, red light has been reported to reduce photosynthetic efficiency, leading to photodamage after prolonged exposure. This phenomenon of spectral deficiency is called "red light syndrome" and leads to a higher nonphotochemical energy loss in PSII (Trouwborst *et al.* 2016).

It is important to note that, in all the aforementioned studies, the light intensity reported was relatively low, at approximately 200 μmol(photon) m^{-2} s^{-1}. This could potentially lead to an underestimation of the effect of spectral quality on leaf development and, consequently, on the photosynthetic apparatus (Liu *et al.* 2011, Trouwborst *et al.* 2016, Fang *et al.* 2021, Trojak *et al.* 2022). Furthermore, in all of these studies, the light intensity remained constant, even in cases of different light spectra. Given that the energy of a photon is contingent on its wavelength, if the number of photons remains constant while their wavelengths undergo alteration, the total energy over time also undergoes a change because energy decreases as wavelength increases. Consequently, plants cultivated under red light receive a lower energy flux at equivalent photon flux compared to those grown under blue light (Nobel 2009). To the best of our knowledge, no research has been conducted on how leaves developed under different light spectra respond photosynthetically to the same amount of light energy.

To understand the adaptation of plants to diverse light environments, it is imperative to conduct experiments that replicate the high energy levels required by the plant species under investigation. Furthermore, it is essential to maintain constant energy flux, photoperiod, and growing time, while varying spectral quality (Quero *et al*. 2019, Walter and Schöbel 2023). Taking this experimental requirement into consideration, the present study aimed to evaluate the effect of four developmental light environments, differing in spectral quality (white light, white light enriched with red, blue light, and red light), under equal energy flux, on PSII energy partitioning in two soybean (*Glycine max* [L.] Merr.) genotypes.

Materials and methods

Plant materials, seedling growing conditions, and plant performance evaluation: Two commercial soybean (*Glycine max* [L.] Merr.) genotypes, DON MARIO 6.8i (DM68i) and GENESIS 5601 (G5601), were used in this study. G5601 is a key cultivar in the Uruguayan breeding program and represents local germplasm variability, whereas DM68i is among the most widely cultivated genotypes in Uruguay. Both genotypes have been previously characterized for their responses to water deficit, showing contrasting behaviors (unpublished data).

Plants were grown in 0.5-L pots filled with a mix of sand:vermiculite (1:1). Three seeds per pot were sown, and after seven days, only the healthiest seedling was chosen to continue the experiment. The seedlings' homogeneity was carefully analyzed to avoid any interference related to their developmental phenotype. Plants were watered

with *B&D* medium (Broughton and Dilworth 1971) supplemented with 5 mM KNO_3 every two days, keeping the substrate at field capacity. To evaluate the plant performance during light treatments, plant transpiration was determined by gravimetry (Fig. 1S, *supplement*). For this, each pot was watered to field capacity and weighed every day in the morning. The pot mass before watering was subtracted from that at field capacity, so the result corresponded to the transpiration of each plant. Each pot had a bottle cap to avoid soil water evaporation (Fig. 1S).

Light treatments and plant growing conditions: The plants were grown in a chamber illuminated by metal halide lamps (MH) until they reached the second trifoliate leaf stage (Fehr and Caviness 1977). The environmental condition of this chamber is described in Table 1S (*supplement*). Afterward, plants were transferred to a chamber for different light treatments (Fig. 1S) until they reached the third trifoliate leaf stage (Fehr and Caviness 1977). A photoperiod of 16/8 h (light/dark) was applied. Plants were maintained at 22–25°C, 40–50% relative humidity (RH), and a vapor pressure deficit (VPD) of 0.90–2.17 kPa. Four light treatments were carried out: MH-white light (WL), LED-red light-enriched white light (RWL), LED-blue light (BL), and LED-red light (RL). Table 2S (*supplement*) describes the environmental conditions of each light treatment during the third trifoliate leaf development stage.

The implementation of all light treatments was conducted utilizing custom-built in-house lighting systems. WL was constructed with metal halide lamps, while RWL, BL, and RL were built with LED lighting. Plants were grown under the same light conditions (WL) until the second trifoliate leaf stage, to assess the effect of light spectral quality exclusively on the development of the third trifoliate leaf. LED lights were built using constant current LED drivers with 0–10 V control to adjust their intensity and match the energy flux despite the different spectral compositions. The RWL spectrum was generated with a light system built using LED modules, *Samsung Horticulture Module*, which has white LEDs *Samsung LM301H* and some red (630 nm) *Samsung LH351H* (Fig. 2S, *supplement*). BL and RL spectra were generated with a light system equipped with custom LED modules with seven single color LEDs *Osram OSLON SSL* covering the PAR spectrum. The intensity of each color is controlled individually. In the case of BL light, deep blue (455 nm) and blue (470 nm) LEDs were on. In the RL spectrum, amber (617 nm), red (623 nm), and hyper red (640 nm) were on (Fig. 2S).

The photosynthetically active radiation (PAR) energy flux in the four treatments was between 137–141 J s^{-1} m^{-2} (Table 3S, *supplement*) and was defined according to the WL treatment. As seen in Fig. 1, the spectral distribution differed within light treatments. The WL and RWL treatments operated through the entire photosynthetically active spectrum (400–700 nm), where RWL had enrichment of its energy in the red band (Δλ7) compared to WL (Table 3S). The BL treatment had wavelengths between 400 and 560 nm (Δλ2, Δλ3, Δλ4; Table 3S).

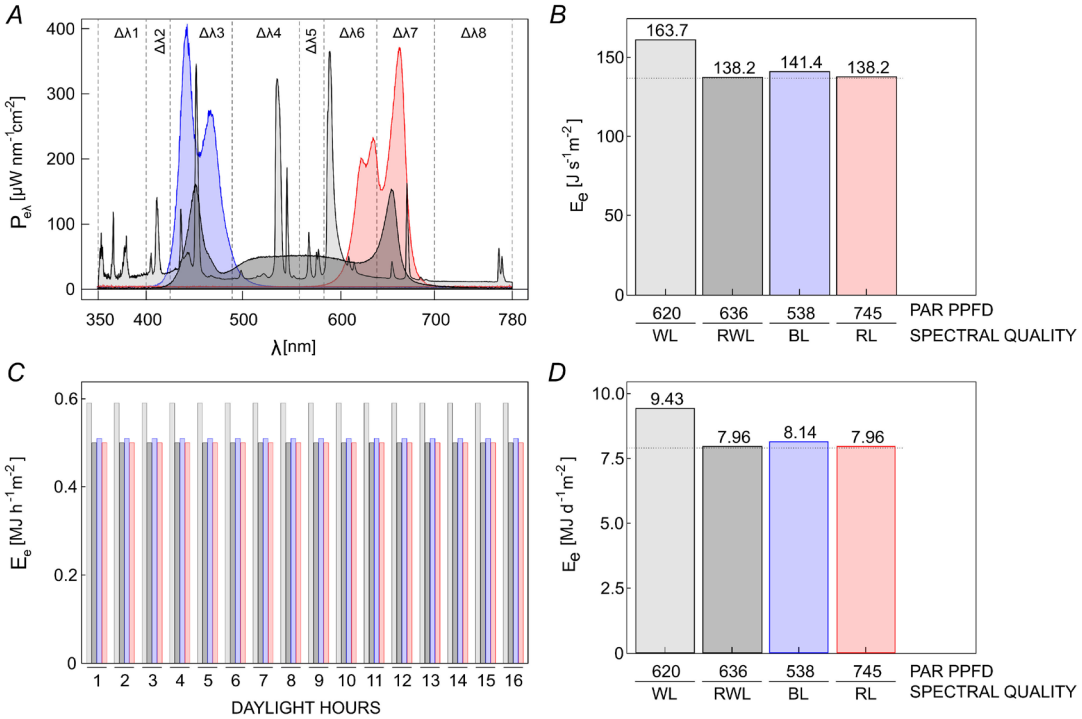

Fig. 1. Light treatments description: spectral quality, photon flux density, and energy. (*A*) Spectral distributions of the four light treatments depicted as spectral power ($P_{e\lambda}$) as a function of wavelength (λ). Δλ is $\lambda_i - \lambda_{i-1}$ as depicted in Table 3S. (*B*) Energy flux (E_e) and photosynthetic photon flux density (PPFD) of photosynthetically active radiation (PAR) of the four light treatments. The area under the curve of each light treatment represents its total E_e. (*C*) E_e per hour received per m^2 of leaf during the daylight hours. (*D*) E_e received by the plant during a day. *The dotted line* indicates the E_e received from PAR radiation only.

The RL treatment had wavelengths in the 585–700 nm range (Δλ6, Δλ7; Table 3S).

The E_e received by the plants under BL and RL was almost the same as under the RWL treatment (Fig. 1, Table 3S). It is noteworthy that the E_e of the PAR region of the three aforementioned treatments is equivalent to that emitted in the PAR region of the WL treatment, which utilizes a metal halide lamp as its light source (Fig. 1, Table 3S). In BL, most of the E_e was concentrated in the interval 425–490 nm of the PAR spectrum (Δλ3; Fig. 1, Table 3S), which represented 94.8% of all the PAR E_e received by the plant in that treatment. In the case of RL, most of the E_e was concentrated between 585–700 nm of the PAR spectrum (Δλ6 and Δλ7; Fig. 1, Table 3S). In these intervals, 99.3% of all PAR E_e received by the plant in that treatment was concentrated. On the other hand, metal halide lamps emit within the 350–400 nm and 700–780 nm ranges, falling outside the PAR spectrum (Δλ1 and Δλ8; Fig. 1, Table 3S). The total E_e emitted in these intervals accounts for 15.8% (9% Δλ1 and 6.8% Δλ8) of the E_e emitted in the entire incident spectrum (350–80 nm; Table 3S). As indicated by the established photoperiod (16/8) in this study, the PAR E_e emitted by the LED systems (RWL, BL, RL treatments) and the metal halide lamp (WL treatment) was approximately 8 MJ d^{-1} m^{-2} (Fig. 1*D*). In the WL treatment, the energy contribution from the non-PAR region of the spectrum was 1 MJ d^{-1} m^{-2} more than the LED treatments, in which the energy outside the PAR region is very low.

Wavelength intervals were defined according to Nobel (2009). The spectrum and light intensity of all light treatments were measured using a spectroradiometer (*USB2000+* spectrometer, *Ocean Optics*, Duiven, The Netherlands) calibrated against a standard light source supplied by the equipment.

Plant morphology measurements: Plant morphology was evaluated at the second trifoliate leaf stage using three traits: (*1*) plant height, (*2*) third internode length, and (*3*) third trifoliate leaf angle. Measurements were obtained from photographs of each plant using *Fiji* software (Rueden *et al.* 2017). The third trifoliate leaf angle was defined relative to a horizontal axis originating at the third trifoliate node and orthogonal to the stem (Fig. 3S, *supplement*).

Energy partitioning: quenching and relaxation analyses: Chlorophyll fluorescence traces of the third trifoliate leaf were measured *in vivo* using a PAM Chl fluorometer (*FMS1*, *Hansatech*, King's Lynn, UK). Fig. 4S (*supplement*) shows three well-differentiated phases during fluorescence induction (F) of PSII: initial phase, quenching analysis, and relaxation analysis. The fluorometer utilized in this study employs a halogen lamp as its light source, emitting nonmonochromatic actinic light. Therefore, the actinic light used for PSII excitation, referred to as defined spectrum actinic light (DSAL), was defined as reported by Quero *et al.* (2021) (Fig. 4S). In the quenching phase, three different DSAL intensities were used [200, 425, and 850 µmol(photon) m^{-2} s^{-1}].

The quantification of energy partition in PSII was determined by the quantum yield of three de-excitation processes using the chlorophyll fluorescence parameters (Lazár 2015, Quero *et al.* 2021). This analysis is based on the idea that the sum of all the de-excitation processes of the energy absorbed by PSII is equal to 1 (Demmig-Adams *et al.* 1996, Hendrickson *et al.* 2004, Logan *et al.* 2014): $\Phi_{PSII} + \Phi_{NPQ} + \Phi_{NO} = 1$, where Φ_{PSII} is the quantum yield of PSII, Φ_{NPQ} is the quantum yield of nonphotochemical quenching, and Φ_{NO} is the quantum yield of constitutive nonregulatory (basal or dark) nonphotochemical dissipation processes. Appendix lists all quantum yield parameters used in this study with their definitions, relationships, and references. The mathematical development performed to obtain the efficiency parameters from the fluorescence quenching analysis is shown in Data 1S (*supplement*).

Experimental design and statistical analysis: A pot with one plant represented an experimental unit. There were four biological replicates ($n = 4$) per soybean genotype and light treatment. A completely random design was applied for each treatment.

A factorial linear model was used for each parameter. The factors were light treatment (LT), genotype (G), and DSAL. Double and triple interactions among factors were tested. The triple interaction with DSAL effects was not significant (Data 1S and Table 4S, *supplement*). Therefore, a model with principal effects LT, G, and DSAL, and double interactions, was fitted and used for statistical analysis.

The general linear model was: $Y_{ijk} = \mu + LT_i + DSAL_j + G_k + (G \times LT)_{ki} + (G \times DSAL)_{kj} + (LT \times DSAL)_{ij} + error_{ijk}$, where µ is a constant, LT_i is the effect of light treatment *i*-level, $DSAL_j$ is the effect of defined spectrum actinic light *j*-level, G_k is the effect of genotype *k*-level, $(G \times LT)_{ki}$ is the interaction effect of genotype *k*-level and light treatment *i*-level, $(G \times DSAL)_{kj}$ is the interaction effect of genotype *k*-level and effect of defined spectrum actinic *j*-level, $(LT \times DSAL)_{ij}$ is the interaction effect of light treatment *i*-level and the effect of defined spectrum actinic light *j*-level. And $error_{ijk}$ is the error term.

An analysis of variance (*ANOVA*) was used to test the differences and interactions among G, LT, and DSAL (Table 5S, *supplement*). Statistical analysis of morphological variables is detailed in Data 2S (*supplement*) and Table 6S (*supplement*).

Differences between the means were tested by orthogonal contrast analyses ($P \leq 0.05$). All statistical analyses were done in *R* using the *stats* package (R Core Team 2023). The model was adjusted using the *lme4* package (Bates *et al.* 2015). The best linear unbiased estimators (BLUEs) and the contrast analyses were performed using the *emmeans* package (Lenth 2024).

Spectral susceptibility index: For each energy partitioning parameter, a spectral susceptibility index (SSI) was calculated through the following equation:

$$SSI = \left(\frac{\Phi_{LTi} - \Phi_{LTref}}{\Phi_{LTref}} \right) \times 100$$

where Φ_{LTi} is the quantum yield value of energy partitioning parameters at the light treatment with a spectral quality i (LTi) and Φ_{LTref} is the quantum yield of energy partitioning parameters at the light treatment whose spectral quality is used as a reference (LTref). The SSI is an index of percentage variation that allows comparing the effects of spectral quality on the energy partitioning parameters of PSII. A positive SSI value indicates that LTi causes an increase in the parameter under analysis compared to the effect of LTref on that parameter. Following the same reasoning, a negative value of SSI indicates that LTi decreases the value of the analyzed parameter compared to the effect of LTref on the same parameter. If the effect of LTi is equal to the effect of LTref on a parameter, the SSI value is zero. In this study, the RWL treatment was used as the LTref (Fig. 1, Table 3S).

The RWL treatment was chosen as the reference treatment (LTref) for two main reasons: (*1*) it allows the evaluation of two different white-light technologies, metal halide lamps (WL) *versus* LEDs (RWL), and (*2*) it enables comparisons within LED technology regarding the effects of spectral deficiencies in the PAR range.

Results

Soybean plant development in different light environments: Daily transpiration rate (Fig. 1S) was used to monitor plants' physiological status during different light treatments. The average accumulated transpiration during the third trifoliate leaf development period in the white light treatments was 409 and 300 g(H_2O) for WL and RWL, respectively. In BL and RL, the average accumulated transpiration during the third trifoliate leaf development period was 315 and 311 g(H_2O), respectively, just above the RWL value. No statistically significant differences in plant height were observed at the second trifoliate stage (15–18 cm), before the initiation of the light treatments (Data 2S, Table 6S).

In contrast, the length of the third internode was significantly affected by spectral quality. The maximum length was recorded under RL (6.9 cm). Plants exposed to WL and BL reached 6.1 and 5.3 cm, respectively, with no significant difference between these treatments (Data 2S, Table 6S). The shortest internodes were observed under RWL (≈3.8 cm), differing significantly from WL and RL, but not from BL (Table 6S). Spectral quality also influenced the angle of the third trifoliate leaf, with mean values ranging from 7° to 37°. No genotype-related differences were detected for either the third internode length or the trifoliate leaf angle (Table 6S).

The third trifoliate developed faster in WL treatment compared to the LED treatments for both genotypes. Specifically, the genotype DM68i under WL conditions required 9 d (84.9 MJ m^{-2}) to develop the third trifoliate, while G5601 required 8 d (75.4 MJ m^{-2}). In contrast, under the RWL condition, DM68i required 15 d (119.4 MJ m^{-2}), while G5601 had a 17-d requirement (135.3 MJ m^{-2}). On the other hand, in BL, the DM68i genotype required 14 d (113.9 MJ m^{-2}), and the G5601 genotype 13 d (105.8 MJ m^{-2}). Finally, in the RL, the DM68i genotype required 14 d (111.4 MJ m^{-2}), while the G5601 genotype required 16 d (127.4 MJ m^{-2}).

PSII quantum yield and its components are affected by spectral light quality during leaf development in a genotype-dependent manner: A significant effect of the main sources of variation, LT, G, and DSAL, was observed for the three quantum yield parameters related to PSII photochemistry (Φ_{PSII}, q_P, and $\Phi_{PSIIpot}$). The G factor explained the highest percentage of the observed variance (Table 5S). The interaction of G with LT was only significant for Φ_{PSII} and $\Phi_{PSIIpot}$. In the case of $\Phi_{PSIIpot}$, the interaction between LT and DSAL was significant and explained 14% of the variance (Table 5S). However, for q_P, the double interactions did not reach statistical significance.

The Φ_{PSII}, q_P, and $\Phi_{PSIIpot}$ of DM68i and G5601 in all light treatments and under different DSAL is depicted in Fig. 2. It was observed that as the intensity of the actinic light increased, Φ_{PSII} decreased in all LT for both genotypes (Fig. 2*A*,*D*).

In order to examine the impact upon the photochemistry of PSII of elevated (Δλ1; Table 3S) and reduced energy (Δλ8; Table 3S) intervals, situated beyond the PAR region, the energy partitioning between the WL and RWL treatments was compared. In both genotypes, Φ_{PSII} values were significantly higher in WL than those observed under the RWL treatment for all DSAL levels (Fig. 2*A*,*D*; Table 7S, *supplement*). In DM68i, the SSI increases were 28, 48, and 60% at 200, 425, and 850 µmol(photon) m^{-2} s^{-1}, respectively, whereas for G5601 the increases were 39, 77, and 96% at 200, 425, and 850 µmol(photon) m^{-2} s^{-1}, respectively (Table 1). Notably, the increase in SSI between the WL and RWL treatments is greater as the level of excitation over PSII increases. This increase is further accentuated in G5601 relative to DM68i (Table 1).

q_P and $\Phi_{PSIIpot}$ exhibited a marked increase in WL compared to RWL for both genotypes (Fig. 2*B*,*C*,*E*,*F*). For DM68i, the SSI increases in q_P were 19, 31, and 52% at 200, 425, and 850 µmol(photon) m^{-2} s^{-1}, respectively (Table 1). For the G5601, the SSI increases were 23, 40, and 63% at 200, 425, and 850 µmol(photon) m^{-2} s^{-1}, respectively (Table 1). In the case of $\Phi_{PSIIpot}$, the SSI values for DM68 at WL were 3, 12, and 4% at 200, 425, and 850 µmol(photon) m^{-2} s^{-1}, respectively. For G5601, the SSI increases in $\Phi_{PSIIpot}$ were 16, 23, and 19% at 200, 425, and 850 µmol(photon) m^{-2} s^{-1}, respectively (Table 1).

In order to study the effect of the spectral deficiency within the PAR radiation range, the effects of the BL and RL treatments on Φ_{PSII} were compared with respect to the RWL treatment. A comparison of the effects of BL and RWL treatments on Φ_{PSII} demonstrated a statistically significant difference only for G5601 at 200 and 425 µmol m^{-2} s^{-1}. At these DSAL levels, comparing BL against RWL, the SSI values were 16 and 28% at 200 and 425 µmol(photon) m^{-2} s^{-1}, respectively (Fig. 2*D*, Table 1). Conversely, a significant difference between RL and RWL values was observed in DM68i only at 850 µmol(photon)

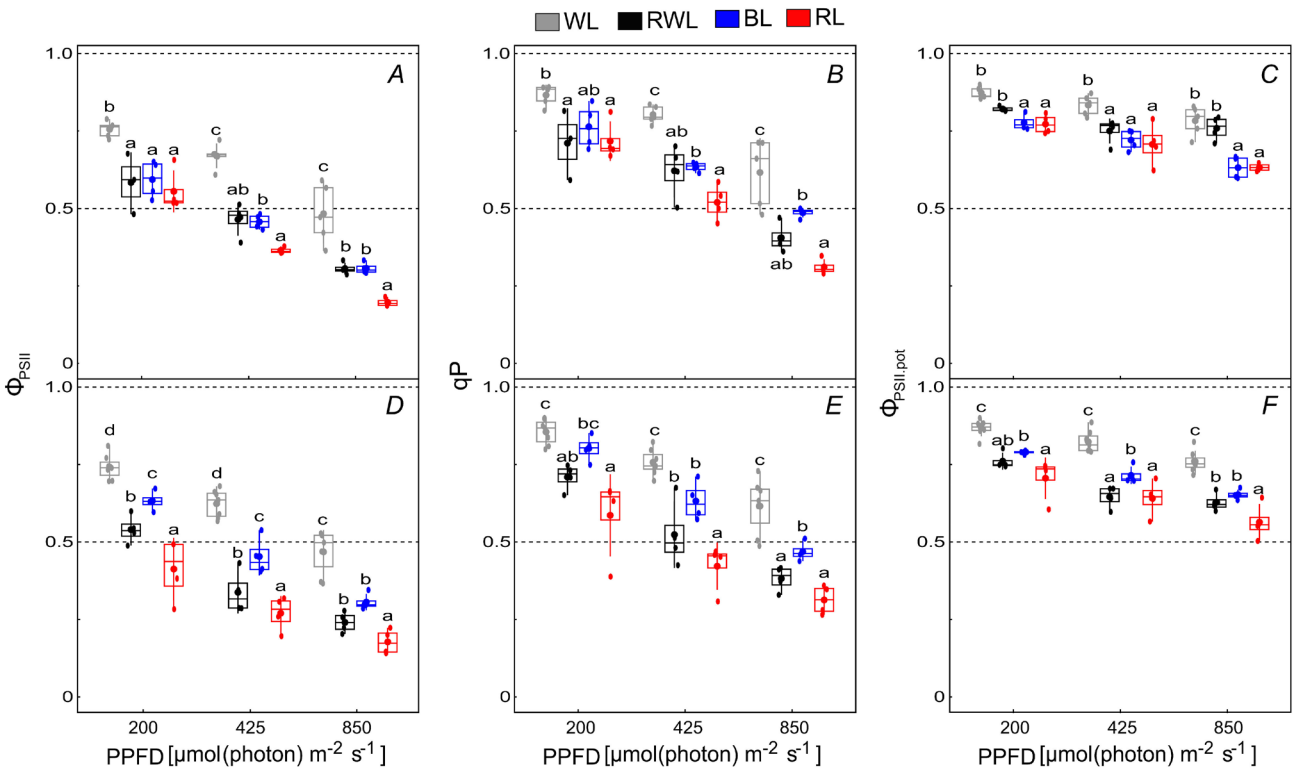

Fig. 2. Quantum yield of PSII parameters under different DSAL conditions for two soybean genotypes. (*A*,*B*,*C*) Φ_{PSII}, q_P, and $\Phi_{PSIIpot}$ for DM68i soybean genotype, respectively. (*D*,*E*,*F*) Φ_{PSII}, q_P, and $\Phi_{PSIIpot}$ for G5601 soybean genotype, respectively. Φ_{PSII} – quantum yield of PSII; q_P – percentage of the open reaction centers; $\Phi_{PSIIpot}$ – the maximum quantum yield of PSII if all reaction centers were open. WL – MH-white light; RWL – LED-red light-enriched white light; BL – LED-blue light; RL – LED-red tight; DSAL – defined spectrum actinic light. *Different letters* indicate significant differences between light treatments at the same DSAL intensity for each genotype.

Table 1. Spectral susceptibility index for PSII quantum yield and its components for two soybean genotypes under different light treatments. Significant differences (P<0.05) are highlighted in bold. DSAL – defined spectrum actinic light; q_P – fraction of open PSII centers at the time t; Φ_{PSII} – quantum yield of the PSII; $\Phi_{PSIIpot}$ – maximal quantum yield of PSII photochemistry for the light-adapted state.

Light treatment	Genotype	Φ_{PSII}			q_P			$\Phi_{PSIIpot}$		
		DSAL [µmol m^{-2} s^{-1}]								
		200	425	850	200	425	850	200	425	850
WL *vs.* RWL	DM68i	**28%**	**48%**	**60%**	**19%**	**31%**	**52%**	3%	**12%**	4%
	G5601	**39%**	**77%**	**96%**	**23%**	**40%**	**63%**	**16%**	**23%**	**19%**
BL *vs.* RWL	DM68i	2%	2%	–20%	7%	5%	15%	**–8%**	–4%	**–15%**
	G5601	**16%**	**28%**	33%	**14%**	15%	**29%**	5%	**10%**	0%
RL *vs.* RWL	DM68i	–13%	–18%	**–26%**	–7%	–14%	–15%	**–8%**	–5%	**–14%**
	G5601	**–16%**	**–26%**	**–38%**	–10%	–22%	–24%	–5%	–1%	**–13%**

m^{-2} s^{-1}, whereas in G5601 this difference was evident at all DSAL levels (Fig. 2*D*). In the case of DM68i, the SSI value was –26% when comparing RL against RWL, while in G5601, the reductions in Φ_{PSII} due to spectral differences were 16, 26, and 38% at 200, 425, and 850 µmol(photon) m^{-2} s^{-1}, respectively (Table 1).

A comparison of q_P values between BL and RWL treatments revealed significant differences for G5601 at 200 and 850 µmol m^{-2} s^{-1} DSAL. At these levels, the SSI values showed that q_P was 14 and 29% higher for BL at 200 and 850 µmol m^{-2} s^{-1}, respectively. On the other hand, comparing RL and RWL treatments, a significant reduction in q_P (22%) was observed only for G5601 at 425 µmol m^{-2} s^{-1} (Fig. 2*B*,*E*; Table 1).

A subsequent analysis of the $\Phi_{PSIIpot}$ values between the BL and RWL treatments revealed that DM68i exhibited significant reductions of 8 and 15% at 200 and 850 µmol(photon) m^{-2} s^{-1}, respectively, under BL treatment. On the contrary, G5601 exhibited a significant increase of 10% at 425 µmol m^{-2} s^{-1} in BL relative to RWL (Fig. 2*C*,*F*; Table 1). In contrast, a comparison of the effect of RL and RWL treatments on $\Phi_{PSIIpot}$ revealed that in DM68i,

the RL treatment resulted in a significant decrease of 8 and 15% at 200 and 850 µmol(photon) m^{-2} s^{-1}, respectively. For G5601, a significant reduction of 13% in $\Phi_{PSIIpot}$ was observed at 850 µmol m^{-2} s^{-1} (Fig. 2*C*,*F*; Table 1).

Quantum yield of light-induced regulated nonphotochemical quenching processes analysis: A significant effect of LT, G, and DSAL was observed for the three quantum yield parameters related to the inducible thermal dissipation of PSII (Φ_{NPQ}, Φ_{NPQf}, and Φ_{NPQs}). The DSAL factor explains the largest percentage of the observed variance for Φ_{NPQ} and Φ_{NPQf}, while for Φ_{NPQs}, most of the variation is explained by LT. The double interactions G × LT and LT × DSAL were found to be significant for all three parameters. For Φ_{NPQs}, these interactions accounted for more than 40% of the variance (Table 5S).

Fig. 3 shows Φ_{NPQ} and their components as a function of the DSAL intensity. Φ_{NPQ} values increased as the DSAL intensity increased. As shown in Fig. 3, Φ_{NPQ} values are generally determined by the values of Φ_{NPQf} rather than Φ_{NPQs}.

For both genotypes, Φ_{NPQ} exhibited a significant decrease in WL compared to RWL at all DSAL intensities (Fig. 3*A*,*D*). In DM68i, the SSI values were –58, –48, and –22% at 200, 425, and 850 µmol(photon) m^{-2} s^{-1}, respectively. For G5601, the SSI values were –75, –54, and –33% at 200, 425, and 850 µmol(photon) m^{-2} s^{-1}, respectively (Table 2).

In line with the observations made for Φ_{NPQ}, Φ_{NPQf} exhibited a reduction in WL compared to RWL at all DSAL intensities. This response was similar for both genotypes (Fig. 3*B*,*E*). In DM68i, the Φ_{NPQf} reductions were 75, 51, and 17% at 200, 425, and 850 µmol(photon) m^{-2} s^{-1}, respectively. For G5601, the Φ_{NPQf} reductions were 68, 52, and 27% at 200, 425, and 850 µmol(photon) m^{-2} s^{-1}, respectively (Table 2). The Φ_{NPQs} parameter exhibited no relevant values in the energy partitioning of PSII for the WL and RWL treatments (Fig. 3*C*,*F*; Table 7S).

A comparison of the Φ_{NPQ} values of the BL and RWL light environments revealed significant differences in G5601 across all DSAL levels, with SSI values of –35, –28, and –14% at 200, 425, and 850 µmol(photon) m^{-2} s^{-1}, respectively (Fig. 3*A*,*D*; Table 2). For the Φ_{NPQf} component, significant differences were only found in G5601 at 425 µmol m^{-2} s^{-1} and represented a reduction in Φ_{NPQf} of 21% (Fig. 3*B*,*E*; Table 2). Conversely, the values of the Φ_{NPQs} component did not demonstrate significant variations (Fig. 3*C*,*F*).

A comparison of the effects of the RL and RWL treatments on Φ_{NPQ} revealed a significant difference between these treatments for DM68i at 200 µmol(photon)

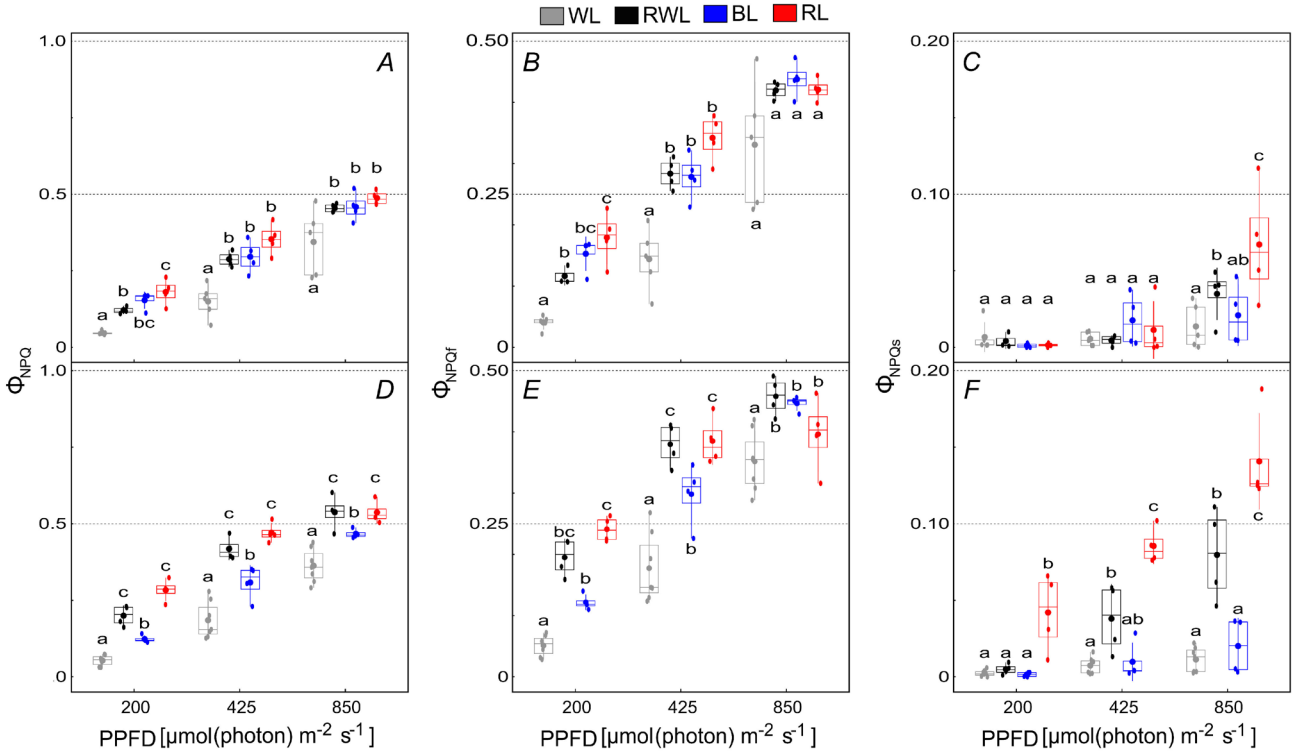

Fig. 3. Inducible energy dissipation quantum yield of two soybean genotypes under four light treatments and three DSAL levels. (*A*,*B*,*C*) Φ_{NPQ}, Φ_{NPQf}, and Φ_{NPQs} for DM68i soybean genotype, respectively. (*D*,*E*,*F*) Φ_{NPQ}, Φ_{NPQf}, and Φ_{NPQs} for G5601 soybean genotype, respectively. Φ_{NPQ} is the quantum yield of light-induced regulated quenching processes. Φ_{NPQf} is the quantum yield of the nonphotochemical quenching related to the regulated energy dissipation in PSII; Φ_{NPQs} is the quantum yield of the nonphotochemical quenching related to the PSII damage caused by photoinhibition. WL – MH-white light; RWL – LED-red light-enriched white light; BL – LED-blue light; RL – LED-red light; DSAL – defined spectrum actinic light. *Different letters* indicate significant differences between light treatments at the same DSAL intensity for each genotype.

Table 2. Spectral susceptibility index for regulated nonphotochemical quenching and its components for two soybean genotypes under different light treatments. † – The value of SSI remains undetermined. The Φ_{NPQs} value is negligible (Table 7S). Significant differences ($P<0.05$) are highlighted in bold. DSAL – defined spectrum actinic light; Φ_{NPQ} – quantum yield of regulatory light-induced nonphotochemical quenching; Φ_{NPQf} – quantum yield of the nonphotochemical quenching of rapid relaxation; Φ_{NPQs} – quantum yield of the nonphotochemical quenching of slow relaxation.

Light treatment	Genotype	Φ_{NPQ}			Φ_{NPQf}			Φ_{NPQs}		
		DSAL [µmol m^{-2} s^{-1}]								
		200	425	850	200	425	850	200	425	850
WL *vs.* RWL	DM68i	**–58%**	**–48%**	**–22%**	**–75%**	**–51%**	–17%	†	†	**–75%**
	G5601	**–75%**	**–54%**	**–33%**	**–68%**	**–52%**	–27%	†	†	**–81%**
BL *vs.* RWL	DM68i	25%	0%	4%	16%	0%	10%	†	†	–50%
	G5601	**–35%**	**–28%**	**–14%**	–26%	**–21%**	–8%	†	–75%	**–71%**
RL *vs.* RWL	DM68i	**58%**	24%	4%	**66%**	17%	–2%	†	†	**75%**
	G5601	35%	16%	1%	15%	2%	–12%	**400%**	**100%**	**100%**

m^{-2} s^{-1} (Fig. 3*A*,*D*). At this intensity level, Φ_{NPQ} exhibited a 58% increase under the RL treatment (Table 2). A similar response was observed for the Φ_{NPQf} component, where the response was 66% higher under RL (Fig. 3*B*,*E*; Table 1). Finally, for the Φ_{NPQs} component, a significant difference was found at 850 µmol(photon) m^{-2} s^{-1} for DM68i. At this DSAL level, the SSI value was 75% when comparing the RL treatment to RWL (Table 2). For G5601, significant differences were observed across all DSAL levels; the SSI values were 400, 100, and 100% at 200, 425, and 850 µmol(photon)m^{-2} s^{-1}, respectively (Table 2).

Quantum yield of the nonphotochemical quenching noninducible processes analysis: Significant effects of LT and G were found on the three quantum yield parameters related to the noninducible thermal dissipation of PSII (Φ_{NO}, Φ_{NOa}, and Φ_{NOb}). The G factor explains the highest percentage of the variance (Table 5S). The DSAL factor exhibited a substantial impact on Φ_{NOb}, accounting for 16% of the variance. The interaction between LT and DSAL was also significant only for Φ_{NOb}, contributing an additional 13% of the variance (Table 5S).

Fig. 4 describes Φ_{NO} and their components as a function of the DSAL intensity. The Φ_{NO} decreased as the DSAL intensity increased in leaves developed under the WL, RWL, and BL treatments (Fig. 4*A*,*D*; Table 7S).

Effect of low- and high-energy wavelengths on the quantum yield of basal energy dissipation in two soybean genotypes: The values of Φ_{NO} were significantly lower in WL than in RWL for DM68i in all DSAL (Fig. 4*A*). The SSI values were –32, –28, and –29% at 200, 425, and 850 µmol(photon) m^{-2} s^{-1}, respectively (Table 3). For G5601, there was only a significant difference at 200 µmol(photon) m^{-2} s^{-1} (Fig. 4*D*), which represents a 22% reduction in the Φ_{NO} (Table 3).

The Φ_{NOa} values were significantly lower in WL than in RWL only for DM68i and at DSAL of 200 and 850 µmol(photon) m^{-2} s^{-1} (Fig. 4*B*). At these levels, the SSI values were 44 and 38% at 200 and 850 µmol(photon) m^{-2} s^{-1}, respectively (Table 3). On the other hand, the Φ_{NOb} values were significantly lower in WL than in RWL for G5601 (Fig. 4*F*) by 21, 30, and 20% at 200, 425, and 850 µmol(photon) m^{-2} s^{-1}, respectively (Table 2).

Effect of spectral deficiency on quantum yield of basal dissipation in two soybean genotypes: The Φ_{NO} values and its component Φ_{NOa} in BL and RWL light environments did not show significant differences at any DSAL (Fig. 4*B*,*E*). The only significant difference was found for Φ_{NOb} of DM68i at 850 µmol(photon) m^{-2} s^{-1} (Fig. 4*C*), where an SSI value of 33% was observed (Table 3). On the other hand, Φ_{NO} in RL and RWL only showed significant differences at 850 µmol(photon) m^{-2} s^{-1} for both genotypes (Fig. 4*A*,*D*), representing an SSI of 29% for DM68i and 32% for G5601. The component Φ_{NOa} showed no significant differences (Fig. 4*B*,*E*). Φ_{NOb} showed significant differences only at 850 µmol m^{-2} s^{-1} in both genotypes (Fig. 4*C*,*F*), representing an SSI of 56% for DM68i and 50% for G5601 (Table 3).

Discussion

Plants remained functionally active until the third trifoliate leaf had developed in all evaluated light environments. This indicates that the development of the third trifoliate leaf was not affected by the spectral quality, particularly in the BL and RL treatments.

Water transpiration was higher in plants grown under WL metal halide lamps than in those grown under LED lamps. Along these lines, Vitale *et al.* (2021) reported lower leaf area in soybean plants grown under LED than those grown under a fluorescent light source. The transpiration rate of plants grown under LED light treatments was found to be similar, despite the different spectral qualities of the treatments, such as BL and RL. This suggests that the energy flux of the light treatment is the main factor affecting transpiration in this study.

At the morphological level, plants grown under the two white light treatments showed differences in internode length and leaf insertion angles. Both parameters were lower in RWL than in WL. This could be due to the higher proportion of red light in RWL (Hirai *et al.* 2006, Huber *et al.* 2021). However, the fact that plants grown

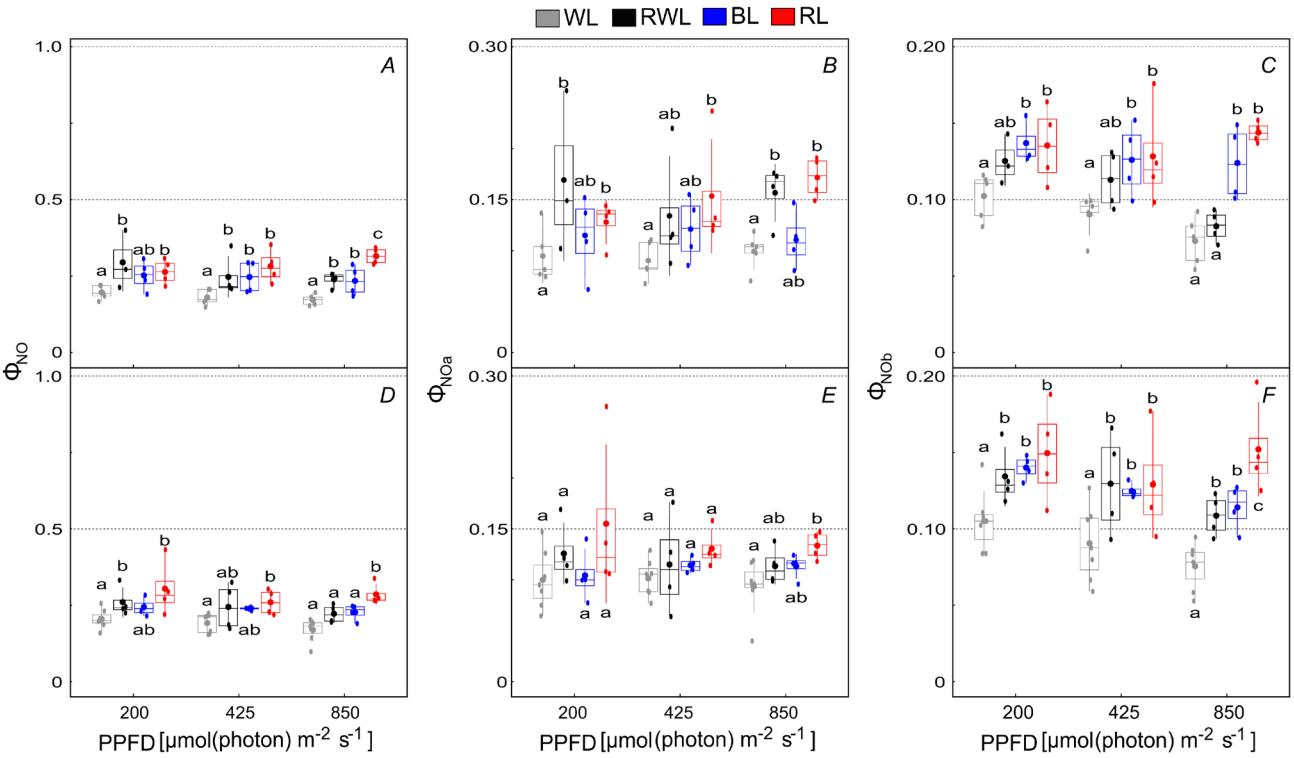

Fig. 4. Basal energy dissipation quantum yield of two soybean genotypes under four light treatments and three DSAL actinic light levels. (*A*,*B*,*C*) Φ_{NO}, Φ_{NOa}, and Φ_{NOb} for DM68i soybean genotype, respectively. (*D*,*E*,*F*) Φ_{NO}, Φ_{NOa}, and Φ_{NOb} for G5601 soybean genotype, respectively. Φ_{NO} reflects the quantum yield of the nonphotochemical quenching constitutive and thermal dissipation processes of fluorescence, Φ_{NOa} is the basal quantum yield of thermal dynamic dissipation within PSII when the Q_As are partially oxidized or partially reduced, and Φ_{NOb} is the basal quantum yield of thermal dissipation within PSII in dark-adapted conditions when Q_A is fully oxidized. WL – MH-white light; RWL – LED-red light-enriched white light; BL – LED-blue light; RL – LED-red light; DSAL – defined spectrum actinic light. *Different letters* indicate significant differences between light treatments at the same DSAL intensity for each genotype.

Table 3. Spectral susceptibility index for basal nonphotochemical quenching and its components for two soybean genotypes under different light treatments. Significant differences ($P<0.05$) are highlighted in bold. DSAL – defined spectrum actinic light; Φ_{NO} – quantum yield of constitutive or basal nonphotochemical quenching; Φ_{NOa} – basal quantum yield of thermal dynamic dissipation within PSII when the pool of Q_As is partially oxidized or partially reduced; Φ_{NOb} – basal quantum yield of thermal dissipation within PSII in dark-adapted conditions when Q_A is fully oxidized.

Light treatment	Genotype	Φ_{NO}			Φ_{NOa}			Φ_{NOb}		
		DSAL [μmol m^{-2} s^{-1}]								
		200	425	850	200	425	850	200	425	850
WL *vs.* RWL	DM68i	**–32%**	**–28%**	**–29%**	**–44%**	–36%	**–38%**	–17%	–18%	–22%
	G5601	**–22%**	–21%	–23%	–23%	–9%	–18%	**–21%**	**–30%**	**–20%**
BL *vs.* RWL	DM68i	–11%	0%	–4%	–31%	–14%	–25%	16%	18%	**33%**
	G5601	–7%	0%	0%	–15%	9%	–9%	0%	–8%	20%
RL *vs.* RWL	DM68i	0%	8%	**29%**	–13%	7%	0%	17%	18%	**56%**
	G5601	7%	13%	**32%**	7%	27%	27%	7%	0%	**50%**

in RL have a larger internode contradicts this result. This apparent contradiction could be explained by considering that the WL treatment had a small far-red peak, whereas RWL did not. These factors could contribute to a lower red/far-red ratio in WL, which could somehow explain the promotion of internode length. The enhancement of stem elongation by low red/far-red ratios is well known in dicotyledonous plant species (Demotes-Mainard *et al.* 2016), which is mainly caused by internode elongation rather than an increased number of internodes (Morgan *et al.* 1980, Demotes-Mainard *et al.* 2016, Hitz *et al.* 2019). On the other hand, when LED light treatments were compared, the internodes of plants grown in RL were larger than those grown in RWL. This is consistent with previous studies on lettuce (Hirai *et al.* 2006) and soybean (Ma *et al.* 2018, Fang *et al.* 2021). The internodal length of

plants grown in BL was also not statistically different from that of plants grown in RWL or RL. There are conflicting results regarding the effects of red light and blue light on morphological traits because they differ between species, genotypes, and growth conditions (Dougher and Bugbee 2004, Hirai *et al*. 2006, Ma *et al*. 2018, Hitz *et al*. 2019).

The implementation of a lighting system specifically designed with LED sources enabled precise analysis of the effects of spectral quality on the development of PSII. The systems developed in this study allowed high levels of PPFD within specific regions of the PAR spectrum. This approach is crucial, as it ensures a constant energy flux across different spectral treatments, minimizing confounding effects between chromatic variation and light intensity. Therefore, it was possible to examine the effects of spectral quality independently of total energy input during leaf development.

To accurately assess the impact of spectral quality on PSII functionality, a thorough characterization of the actinic light used to drive photosynthetic processes was carried out. Accurate spectral characterization is essential for proper interpretation of chlorophyll fluorescence parameters, as previously reported (Terashima *et al.* 2009, Oguchi *et al.* 2011, Zavafer *et al.* 2015b, Quero *et al.* 2019). In this study, energy partitioning processes in PSII were induced by defined DSAL, with intensity experimentally controlled.

Analysis of PSII quantum yield revealed a clear effect of light spectral quality on the functional organization of the photosystem, as widely documented in various species (Brown *et al.* 1995, Yorio *et al.* 2001, Matsuda *et al.* 2004, Ohashi-Kaneko *et al.* 2006, Hogewoning *et al.* 2010b, Lazar *et al.* 2022, Yudina *et al*. 2022). Specifically, results obtained in soybean indicated that PSII functionality is dependent on both genotype and the light quality treatment applied during leaf development. To quantify this differential response, a spectral susceptibility index (SSI) was proposed as a benchmark for evaluating the impact of distinct spectral environments on PSII functional performance.

Experimental data showed that wavelengths beyond the PAR range enhanced PSII operating efficiency. Compared to the reference, RWL treatment, which spanned the entire PAR range, the PSII operating efficiency (Φ_{PSII}) was significantly higher under the broad-spectrum WL condition. Moreover, leaf development was faster under WL than under spectrally restricted LED treatments, with consistent trends across both genotypes tested. These findings align with previous reports indicating that non-PAR wavelengths positively influence photosynthesis and leaf morphogenesis (Nelson and Bugbee 2014, Sena *et al.* 2024). Decomposition of Φ_{PSII} into $\Phi_{PSIIpot}$ and q_P revealed that light treatments had a greater influence on q_P, indicating that spectral quality during development primarily affected PSII functional capacity rather than its maximum photochemical potential.

The effects of spectral deficiency outside the blue range (425–490 nm, BL treatment) on PSII development were null or even positive when compared to RWL of equal energy flux. In DM68i, no differences in Φ_{PSII} were observed under BL. However, under high excitation intensity [850 µmol(photon) m^{-2} s^{-1}], DM68i exhibited a reduction in $\Phi_{PSIIpot}$ which was offset by increased RC openness (q_P). Conversely, PSII from G5601 plants developed under BL showed better performance at low and medium excitation intensities [200 and 425 µmol(photon) m^{-2} s^{-1}]. At 200 µmol(photon) m^{-2} s^{-1}, increased Φ_{PSII} resulted from enhanced RC openness, while at 425 µmol(photon) m^{-2} s^{-1}, the improvement of Φ_{PSII} was due to higher $\Phi_{PSIIpot}$. Several authors have also reported improved PSII operating efficiency under blue light (Hogewoning *et al.* 2010b, Liu *et al.* 2011, Zhang *et al.* 2019, Fang *et al.* 2021).

Regarding Φ_{NPQ}, G5601 grown under BL showed lower values across all DSALs compared to RWL, indicating improved PSII performance. In contrast, no significant differences in NPQ were detected for DM68i under BL. The responses of Φ_{PSII} and Φ_{NPQ} suggest genotype-specific sensitivity to BL, with greater benefits in G5601. Blue light had no significant effect on Φ_{NO} in either genotype. This response may be mediated by a blue-light photosensory pathway that regulates the expression of PSII structural protein genes (Hogewoning *et al.* 2010b) and enzymes involved in chlorophyll synthesis, thereby controlling PSII antenna size (Yudina *et al*. 2022).

PSIIs developed under RL (585–700 nm) showed reduced PSII operability. This negative effect of spectral deficiency outside the red region was attributed to a decrease in $\Phi_{PSIIpot}$, as q_P remained unaffected. Genotypic differences were observed: in DM68i, the reduction in PSII performance (both Φ_{PSII} and $\Phi_{PSIIpot}$) occurred only at the highest DSAL intensity, while G5601 exhibited deficiencies even under low excitation.

The detrimental effects of RL on Φ_{PSII} have been reported in *Lycopersicon esculentum* (Liu *et al.* 2011) and *Solanum lycopersicum* (Zhang *et al.* 2019). In *Glycine max*, Fang *et al.* (2021) observed a decrease in Φ_{PSII} and the percentage of open PSII RCs with increasing red-light proportion (>75%). This condition is commonly referred to as "red light syndrome", characterized by low Φ_{PSII} and high Φ_{NO} (Trouwborst *et al.* 2016).

In this study, leaves grown under RL displayed higher Φ_{NO} than those under other treatments. Notably, it was identified Φ_{NOb} as the main Φ_{NO} component affected by red light syndrome, as both genotypes exhibited higher Φ_{NOb}. Furthermore, photodamage to RCs, quantified by Φ_{NPQs}, was evident under RL. G5601 experienced photodamage at all DSAL intensities, while DM68i was affected only at the highest intensity, confirming genotype-specific sensitivity to red light. When comparing RWL to WL, similar trends were observed: lower Φ_{PSII} and $\Phi_{PSIIpot}$, higher Φ_{NO}, Φ_{NOb}, and Φ_{NPQs}.

In conclusion, we characterized the effects of spectral quality, under a constant energy flux, on PSII functionality during leaf development. Using chlorophyll fluorescence-based energy partitioning at three excitation intensities, we demonstrated that red light environments had the strongest negative impact on PSII operability in both genotypes, consistent with red light syndrome. Common indicators for both genotypes included: reduced Φ_{PSII} and $\Phi_{PSIIpot}$, increased Φ_{NOb}, and greater Φ_{NPQs} photodamage.

G5601 was more susceptible to red light stress but exhibited superior performance under blue light compared to DM68i, highlighting genotype-specific responses to spectral environments.

References

Ahn T.K., Avenson T.J., Peers G. *et al.*: Investigating energy partitioning during photosynthesis using an expanded quantum yield convention. – Chem. Phys. **357**: 151-158, 2009.

Baker N.R.: Chlorophyll fluorescence: a probe of photosynthesis *in vivo*. – Annu. Rev. Plant Biol. **59**: 89-113, 2008.

Bates D., Mächler M., Bolker B., Walker S.: Fitting linear mixed-effects models using lme4. – J. Stat. Softw. **67**: 1-48, 2015.

Broughton W.J., Dilworth M.J.: Control of leghaemoglobin synthesis in snake beans. – Biochem. J. **125**: 1075-1080, 1971.

Brown C.S., Schuerger A.C., Sager J.C.: Growth and photomorphogenesis of pepper plants under red light-emitting diodes with supplemental blue or far-red lighting. – J. Am. Soc. Hortic. Sci. **120**: 808-813, 1995.

Courbier S., Pierik R.: Canopy light quality modulates stress responses in plants. – iScience **22**: 441-452, 2019.

Demmig-Adams B., Adams III W.W., Barker D.H. *et al.*: Using chlorophyll fluorescence to assess the fraction of absorbed light allocated to thermal dissipation of excess excitation. – Physiol. Plantarum **98**: 253-264, 1996.

Demotes-Mainard S., Péron T., Corot A. *et al*.: Plant responses to red and far-red lights, applications in horticulture. – Environ. Exp. Bot. **121**: 4-21, 2016.

Devlin P.F., Christie J.M., Terry M.J.: Many hands make light work. – J. Exp. Bot. **58**: 3071-3077, 2007.

Didaran F., Kordrostami M., Ghasemi-Soloklui A.A. *et al.*: The mechanisms of photoinhibition and repair in plants under high light conditions and interplay with abiotic stressors. – J. Photoch. Photobio. B **259**: 113004, 2024.

Dougher T.A., Bugbee B.: Long-term blue light effects on the histology of lettuce and soybean leaves and stems. – J. Am. Soc. Hortic. Sci. **29**: 467-472, 2004.

Fang L., Ma Z., Wang Q. *et al.*: Plant growth and photosynthetic characteristics of soybean seedlings under different LED lighting quality conditions. – J. Plant Growth Regul. **40**: 668-678, 2021.

Fehr W.R., Caviness C.E.: Stages of Soybean Development. Special Report 80. Pp. 12. Iowa Agricultural Experiment Station, Iowa State University, Ames 1977.

Genty B., Briantais J.-M., Baker N.R.: The relationship between the quantum yield of photosynthetic electron transport and quenching of chlorophyll fluorescence. – BBA-Gen. Subjects **990**: 87-92, 1989.

Hamdani S., Khan N., Perveen S. *et al.*: Changes in the photosynthesis properties and photoprotection capacity in rice (*Oryza sativa*) grown under red, blue, or white light. – Photosynth. Res. **139**: 107-121, 2019.

Hartman G.L., West E.D., Herman T.K.: Crops that feed the World 2. Soybean – worldwide production, use, and constraints caused by pathogens and pests. – Food Secur. **3**: 5-17, 2011.

Hendrickson L., Furbank R.T., Chow W.S.: A simple alternative approach to assessing the fate of absorbed light energy using chlorophyll fluorescence. – Photosynth. Res. **82**: 73-81, 2004.

Hikosaka K., Kato M.C., Hirose T.: Photosynthetic rates and partitioning of absorbed light energy in photoinhibited leaves. – Physiol. Plantarum **121**: 699-708, 2004.

Hirai T., Amaki W., Watanabe H.: Action of blue or red monochromatic light on stem internodal growth depends on plant species. – Acta Hortic. **711**: 345-350, 2006.

Hitz T., Hartung J., Graeff-Hönninger S., Munz S.: Morphological response of soybean (*Glycine max* (L.) Merr.) cultivars to light intensity and red to far-red ratio. – Agronomy **9**: 428, 2019.

Hogewoning S.W., Douwstra P., Trouwborst G. *et al.*: An artificial solar spectrum substantially alters plant development compared with usual climate room irradiance spectra. – J. Exp. Bot. **61**: 1267-1276, 2010a.

Hogewoning S.W., Trouwborst G., Maljaars H. *et al.*: Blue light dose-responses of leaf photosynthesis, morphology, and chemical composition of *Cucumis sativus* grown under different combinations of red and blue light. – J. Exp. Bot. **61**: 3107-3117, 2010b.

Huber M., Nieuwendijk N.M., Pantazopoulou C.K., Pierik R.: Light signalling shapes plant–plant interactions in dense canopies. – Plant Cell Environ. **44**: 1014-1029, 2021.

Kasajima I., Takahara K., Kawai-Yamada M.. Uchimiya H.: Estimation of the relative sizes of rate constants for chlorophyll de-excitation processes through comparison of inverse fluorescence intensities. – Plant Cell Physiol. **50**: 1600-1616, 2009.

Kochetova G.V., Avercheva O.V., Bassarskaya E.M., Zhigalova T.V.: Light quality as a driver of photosynthetic apparatus development. – Biophys. Rev. **14**: 779-803, 2022.

Kramer D.M., Johnson G., Kiirats O., Edwards G.E.: New fluorescence parameters for the determination of Q_A redox state and excitation energy fluxes. – Biol. Chem. **79**: 209-218, 2004.

Lazar D., Stirbet A., Björn L.O., Govindjee G.: Light quality, oxygenic photosynthesis and more. – Photosynthetica **60**: 25-58, 2022.

Lazár D.: Parameters of photosynthetic energy partitioning. – J. Plant Physiol. **175**: 131-147, 2015.

Lenth R.V.: emmeans: Estimated Marginal Means, aka Least-Squares Means. *R* package version 1.10.0, 2024. *Available at*: https://CRAN.R-project.org/package=emmeans.

Liu X.Y., Chang T.T., Guo S.R. *et al.*: Effect of different light quality of LED on growth and photosynthetic character in cherry tomato seedling. – Acta Hortic. **907**: 325-330, 2011.

Logan B.A., Demmig-Adams B., Adams III W.W., Bilger W.: Context, quantification, and measurement guide for non-photochemical quenching of chlorophyll fluorescence. – In: Demmig-Adams B., Garab G., Adams III W., Govindjee (ed.): Non-Photochemical Quenching and Energy Dissipation in Plants, Algae and Cyanobacteria. Advances in Photosynthesis and Respiration. Pp. 187-201. Vol. 40. Springer, Dordrecht 2014.

Ma Z., Nian H., Luo S. *et al.*: Growth responses of soybean (*Glycine max* L.) seedlings as affected by monochromic or mixture radiation provided by light-emitting diode. – IFAC-PapersOnLine **51**: 770-777, 2018.

Matsuda R., Ohashi-Kaneko K., Fujiwara K. *et al.*: Photosynthetic characteristics of rice leaves grown under red light with or without supplemental blue light. – Plant Cell Physiol. **45**: 1870-1874, 2004.

Maxwell K., Johnson G.N.: Chlorophyll fluorescence – a practical guide. – J. Exp. Bot. **51**: 659-668, 2000.

Morgan D.C, O'Brien T., Smith H.: Rapid photomodulation of stem extension in light-grown *Sinapis alba* L. – Planta **150**: 95-101, 1980.

Nelson J.A., Bugbee B.: Economic analysis of greenhouse lighting: light emitting diodes *vs.* high intensity discharge fixtures. – PLoS ONE **9**: e99010, 2014.

Nobel P.S.: Physicochemical and Environmental Plant Physiology. Fourth Edition. Pp. 604. Academic Press, Oxford 2009.

Oguchi R., Douwstra P., Fujita T. *et al.*: Intra-leaf gradients of photoinhibition induced by different color lights: implications for the dual mechanisms of photoinhibition and for the application of conventional chlorophyll fluorometers. – New Phytol. **191**: 146-159, 2011.

Ohashi-Kaneko K., Matsuda R., Goto E. *et al.*: Growth of rice plants under red light with or without supplemental blue light. – Soil Sci. Plant Nutr. **52**: 444-452, 2006.

Oxborough K., Baker N.R.: Resolving chlorophyll *a* fluorescence images of photosynthetic efficiency into photochemical and non-photochemical components – calculation of qP and Fv'/Fm' without measuring Fo'. – Photosynth. Res. **54**: 135-142, 1997.

Quero G., Bonnecarrère V., Fernández S. *et al.*: Light-use efficiency and energy partitioning in rice is cultivar dependent. – Photosynth. Res. **140**: 51-63, 2019.

Quero G., Bonnecarrère V., Simondi S. *et al.*: Genetic architecture of photosynthesis energy partitioning as revealed by a genome-wide association approach. – Photosynth. Res. **150**: 97-115, 2021.

R Core Team: *R*: A Language and Environment for Statistical Computing. *R* Foundation for Statistical Computing, Vienna, Austria, 2023. *Available at*: https://www.R-project.org/.

Rueden C.T., Schindelin J., Hiner M.C. *et al.*: ImageJ2: ImageJ for the next generation of scientific image data. – BMC Bioinformatics **18**: 529, 2017.

Sena S., Kumari S., Kumar V., Husen A.: Light emitting diode (LED) lights for the improvement of plant performance and production: a comprehensive review. – Curr. Res. Biotechnol. **7**: 100184, 2024.

Skálová H., Krahulec F., During H.J. *et al.*: Grassland canopy composition and spatial heterogeneity in the light quality. – Plant Ecol. **143**: 129-139, 1999.

Stirbet A., Lazár D., Guo Y., Govindjee G.: Photosynthesis: basics, history and modelling. – Ann. Bot.-London **126**: 511-537, 2020.

Takemiya A., Inoue S.I., Doi M. *et al.*: Phototropins promote plant growth in response to blue light in low light environments. – Plant Cell **17**: 1120-1127, 2005.

Terashima I., Fujita T., Inoue T. *et al.*: Green light drives leaf photosynthesis more efficiently than red light in strong white light: revisiting the enigmatic question of why leaves are green. – Plant Cell Physiol. **50**: 684-697, 2009.

Trivellini A., Toscano S., Romano D., Ferrante A.: LED lighting to produce high-quality ornamental plants. – Plants-Basel **12**: 1667, 2023.

Trojak M., Skowron E., Sobala T. *et al.*: Effects of partial replacement of red by green light in the growth spectrum on photomorphogenesis and photosynthesis in tomato plants. – Photosynth. Res. **151**: 295-312, 2022.

Trouwborst G., Hogewoning S.W., van Kooten O. *et al.*: Plasticity of photosynthesis after the 'red light syndrome' in cucumber. – Environ. Exp. Bot. **121**: 75-82, 2016.

Vitale E., Velikova V., Tsonev T. *et al.*: The interplay between light quality and biostimulant application affects the antioxidant capacity and photosynthetic traits of soybean (*Glycine max* L. Merrill). – Plants-Basel **10**: 861, 2021.

Walter A., Schöbel H.: Shed light on photosynthetic organisms: a physical perspective to correct light measurements. – Photosynth. Res. **156**: 325-336, 2023.

Wang J., Lu W., Tong Y., Yang Q.: Leaf morphology, photosynthetic performance, chlorophyll fluorescence, stomatal development of lettuce (*Lactuca sativa* L.) exposed to different ratios of red light to blue light. – Front. Plant Sci. **7**: 250, 2016.

Yang L.Y., Wang L.T., Ma J.H. *et al.*: Effects of light quality on growth and development, photosynthetic characteristics and content of carbohydrates in tobacco (*Nicotiana tabacum* L.) plants. – Photosynthetica **55**: 467-477, 2017.

Yorio N.C., Goins G.D., Kagie H.R. *et al.*: Improving spinach, radish, and lettuce growth under red light-emitting diodes (LEDs) with blue light supplementation. – HortScience **36**: 380-383, 2001.

Yudina L., Sukhova E., Mudrilov M. *et al.*: Ratio of intensities of blue and red light at cultivation influences photosynthetic light reactions, respiration, growth, and reflectance indices in lettuce. – Biology **11**: 60, 2022.

Zavafer A.: A theoretical framework of the hybrid mechanism of photosystem II photodamage. – Photosynth. Res. **149**: 107-120, 2021.

Zavafer A., Cheah M.H., Hillier W. *et al.*: Photodamage to the oxygen evolving complex of photosystem II by visible light. – Sci. Rep.-UK **5**: 16363, 2015a.

Zavafer A., Chow W.S., Cheah M.H.: The action spectrum of Photosystem II photoinactivation in visible light. – J. Photoch. Photobio. B **152**: 247-260, 2015b.

Zhang M., Liu S., Wang Z. *et al.*: Progress in soybean functional genomics over the past decade. – Plant Biotechnol. J. **20**: 256-282, 2022.

Zhang Y., Kaiser E., Zhang Y. *et al.*: Red/blue light ratio strongly affects steady-state photosynthesis, but hardly affects photosynthetic induction in tomato (*Solanum lycopersicum*). – Physiol. Plantarum **167**: 144-158, 2019.

Zheng L., Van Labeke M.-C.: Long-term effects of red- and blue-light emitting diodes on leaf anatomy and photosynthetic efficiency of three ornamental pot plants. – Front. Plant Sci. **8**: 917, 2017.

Zheng L., Van Labeke M.-C.: Effects of different irradiation levels of light quality on *Chrysanthemum*. – Sci. Hortic.-Amsterdam **233**: 124-131, 2018.

Appendix. The quantum yield parameters.

Parameter	Definition	Reference
$\Phi_{PSII} = (F_m' - F_t)/F_m'$	PSII quantum yield as a function of time t.	Genty *et al*. 1989
$\Phi_{PSIIpot} = (F_m' - F_0')/F_m'$	It is an estimation of Φ_{PSII} if all PSII RC are open.	Oxborough and Baker 1997
$q_P = (F_m' - F_t)/(F_m' - F_0)$	The q_P is defined as photochemical quenching or the proportion of open PSII RC.	Maxwell and Johnson 2000, Kramer *et al.* 2004
$\Phi_{PSII} = \Phi_{PSIIpot} \times q_P$		
$\Phi_{NPQ} = F_t[(1/F_m') - (1/F_m)]$	Quantum yield of non-basal light-induced non-photochemical quenching.	Maxwell and Johnson 2000, Baker 2008
$\Phi_{NPQf} = F_t[(1/F_m') - (1/F_m'')]$	Quantum yield of the nonphotochemical quenching of rapid relaxation. It is related to the regulated energy dissipation in PSII.	Kasajima *et al*. 2009, Ahn *et al*. 2009

$\Phi_{NPQs} = F_t[(1/F_m'') - (1/F_m)]$	Quantum yield of the nonphotochemical quenching of slow relaxation. It is related to the PSII damage caused by photoinhibition.	Kasajima *et al*. 2009, Ahn *et al*. 2009
$\Phi_{NPQ} = \Phi_{NPQf} + \Phi_{NPQs}$		
$\Phi_{NO} = F_t/F_m$	Quantum yield of constitutive or basal nonphotochemical quenching.	Kasajima *et al*. 2009, Ahn *et al*. 2009
$\Phi_{NOa} = (F_t - F_0')/F_m$	Basal quantum yield of thermal dynamic dissipation within PSII when the pool of plastoquinone A (Q_A) is partially oxidized or partially reduced.	Hikosaka *et al.* 2004
$\Phi_{NOb} = F_0'/F_m$	Basal quantum yield of thermal dissipation within PSII in dark-adapted conditions when Q_As are fully oxidized.	Hikosaka *et al.* 2004
$\Phi_{NO} = \Phi_{NOa} + \Phi_{NOb}$		